Am J Physiol Endocrinol Metab 317: E158–E171, 2019.
First published April 30, 2019; doi:10.1152/ajpendo.00521.2018.

RESEARCH ARTICLE | *Role of Gut Microbiota, Gut-Brain and Gut Liver Axes in Physiological Regulation of Inflammation, Energy Balance, and Metabolism*

Gut bacteria are critical for optimal muscle function: a potential link with glucose homeostasis

Kevin Nay,[1,2]* Maxence Jollet,[1]* Benedicte Goustard,[1] Narjes Baati,[1] Barbara Vernus,[1] Maria Pontones,[1] Luz Lefeuvre-Orfila,[2] Claude Bendavid,[3] Olivier Rué,[4] Mahendra Mariadassou,[4] Anne Bonnieu,[1] Vincent Ollendorff,[1] Patricia Lepage,[5] Frédéric Derbré,[2] and Christelle Koechlin-Ramonatxo[1]

[1]*DMEM, University of Montpellier, INRA, Montpellier, France;* [2]*Laboratory "Movement Sport and Health Sciences" EA7470, University of Rennes/ENS Rennes, France;* [3]*Institut NuMeCan, Inserm U1241/CHU Rennes/INRA, Université de Rennes, Rennes, France;* [4]*MaIAGE, INRA, Université Paris-Saclay, Jouy-en-Josas, France; and* [5]*MICALIS, AgroParisTech, INRA, Université Paris-Saclay, Jouy-en-Josas, France*

Submitted 3 December 2018; accepted in final form 9 April 2019

Nay K, Jollet M, Goustard B, Baati N, Vernus B, Pontones M, Lefeuvre-Orfila L, Bendavid C, Rué O, Mariadassou M, Bonnieu A, Ollendorff V, Lepage P, Derbré F, Koechlin-Ramonatxo C. Gut bacteria are critical for optimal muscle function: a potential link with glucose homeostasis. *Am J Physiol Endocrinol Metab* 317: E158–E171, 2019. First published April 30, 2019; doi:10.1152/ajpendo.00521.2018.—Gut microbiota is involved in the development of several chronic diseases, including diabetes, obesity, and cancer, through its interactions with the host organs. It has been suggested that the cross talk between gut microbiota and skeletal muscle plays a role in different pathological conditions, such as intestinal chronic inflammation and cachexia. However, it remains unclear whether gut microbiota directly influences skeletal muscle function. In this work, we studied the impact of gut microbiota modulation on mice skeletal muscle function and investigated the underlying mechanisms. We determined the consequences of gut microbiota depletion after treatment with a mixture of a broad spectrum of antibiotics for 21 days and after 10 days of natural reseeding. We found that, in gut microbiota-depleted mice, running endurance was decreased, as well as the extensor digitorum longus muscle fatigue index in an ex vivo contractile test. Importantly, the muscle endurance capacity was efficiently normalized by natural reseeding. These endurance changes were not related to variation in muscle mass, fiber typology, or mitochondrial function. However, several pertinent glucose metabolism markers, such as ileum gene expression of short fatty acid chain and glucose transporters G protein-coupled receptor 41 and sodium-glucose cotransporter 1 and muscle glycogen level, paralleled the muscle endurance changes observed after treatment with antibiotics for 21 days and reseeding. Because glycogen is a key energetic substrate for prolonged exercise, modulating its muscle availability via gut microbiota represents one potent mechanism that can contribute to the gut microbiota-skeletal muscle axis. Taken together, our results strongly support the hypothesis that gut bacteria are required for host optimal skeletal muscle function.

contractile properties; dysbiosis; maximal aerobic velocity; mitochondrial biogenesis; muscle fatigue

INTRODUCTION

About 10^{14} bacteria live in our gut in symbiosis. This community is now considered as a central organ because of its tremendous impact on human health (17, 37). Indeed, gut microbiota dysbiosis is involved, directly or indirectly, in numerous chronic diseases, such as obesity, type 1 and type 2 diabetes, allergy, and autism (63). The impact of gut microbiota in chronic diseases can be explained by its interactions with the host organs, including brain (21), liver (9), and lung (62).

Recently, the hypothesis of a cross talk between gut microbiota and skeletal muscle has emerged in the literature (5). For example, in mouse models of intestinal chronic inflammation, the restoration of commensal *Escherichia coli* levels efficiently prevents skeletal muscle atrophy (52). Moreover, the recovery of a "healthy" microbiota by synbiotic treatment prolongs survival and reduces cancer proliferation and cachexia development in mouse models of cancer (4, 69). Gut microbiota may also influence the muscle metabolism and fiber phenotype and, consequently, the exercise performance. For instance, after microbiota transplantation from obese or lean pigs, germ-free (GF) mice replicate the fiber characteristics and lipid metabolic profile of the donor's skeletal muscle (70). Interestingly, probiotic supplementation in mice also improves muscle mass, promotes the slow and oxidative muscle phenotype associated with increased muscle endurance, and reduces exercise-induced muscle damage (14, 35). More recently, in vitro experiments showed that microbiota-derived phenolic metabolites found in blood promote muscle glucose uptake in differentiated human skeletal muscle myoblasts in a dose-dependent manner (33).

Considering microbiota as a regulatory element of skeletal muscle function is an innovative idea with significant scientific and socioeconomic consequences. Indeed, loss of muscle function and mass is a risk factor of morbidity and mortality in neuromuscular diseases, and also in many chronic diseases (e.g., cancer cachexia, obesity, diabetes) (24, 40). The identification of the role played by gut microbiota in the skeletal muscle dysfunction related to such chronic diseases could clearly improve the management of these patients. However, the in vivo mechanisms underlying the functional link between

* K. Nay and M. Jollet contributed equally to this work.

Address for reprint requests and other correspondence: C. Koechlin-Ramonatxo, DMEM, Univ Montpellier, INRA, Montpellier, France, 2 place Pierre viala, 34060 Montpellier, France (e-mail: christelle.ramonatxo@supagro.inra.fr).

gut microbiota and skeletal muscle in healthy conditions remain poorly explored. In this context, assessing the effect of microbiota modulation on skeletal muscle function would constitute a significant step forward.

Germ-free mice have been previously used to investigate the functional link between microbiota and different organs (42). However, these mice have developed compensatory mechanisms to the life-long absence of microbiota (25). On the other hand, antibiotic treatment is a recognized procedure to induce short-term gut microbiota depletion for studying its impact on the host organs (56). Finally, another advantage of antibiotic treatment is that it allows the subsequent recovery of healthy gut microbiota through natural reseeding.

The aim of this study was to determine in healthy mice whether gut microbiota affects skeletal muscle. To this purpose, we modulated gut microbiota in healthy mice by antibiotic treatment and natural reseeding. We found that antibiotic-mediated gut microbiota depletion induced a decrease of skeletal muscle endurance. Interestingly, this deleterious effect was entirely normalized by natural reseeding. We also investigated putative mechanisms and discovered that glucose homeostasis is modified by gut microbiota, since we observed that short fatty acid chain and glucose transporter [G protein-coupled receptor (Gpr) 41, sodium/glucose cotransporter 1 (Sglt1)] expression in ileum and glycogen content in muscle were decreased after gut microbiota depletion and normalized after natural reseeding. In summary, our study strongly suggests that the presence of bacteria in the gut influences the skeletal muscle metabolism and function of the host.

MATERIALS AND METHODS

Animal experiments were approved by the Animal Experimentation Ethics Committee (Autorisation de Projet utilisant des Animaux à des Fins Scientifiques no. 2551–2015110311365663) in accordance with the recommendations of the *Guide for the Care and Use of Laboratory Animals* (National Institutes of Health Publication no. 85–23, revised 1996) and according to the European directives (86/609/European Economic Community).

C57BL/6 Mice

C57BL/6 male mice (14 wk old; Charles River) were randomly divided in the following three experimental groups: control group (CTL, $n = 10$), group treated with antibiotics for 21 days (ATB, $n = 10$), and group treated with antibiotics for 10 days followed by natural reseeding for another 11 days (NAT, $n = 9$). Mice were maintained on a 12:12-h dark-light cycle in a temperature-controlled room in individual cages with filter lids and had ad libitum access to food and water. The diet (3,395 kcal/kg) was standardized and identical for all groups (ref. A03, safe diets). It included 69.2% of cereals, 20.2% of vegetal protein, 6.0% of animal protein, and 4.6% of mineral and vitamin cocktail. The following is a general description of the macronutrient composition: 61.3% protein carbohydrates, 25.2% protein, and 13.5% lipids. This diet is currently used in our animal care facility after the birth of mice. Except for running tests, mice were housed in individual standard cages (not wheel cages) and thus were not subjected to daily exercise.

The ATB group received an oral cocktail of broad-spectrum antibiotics (1 mg/ml ampicillin, 5 mg/ml streptomycin, 1 mg/ml colistin, and 45 μg/ml vancomycin in drinking water).

To investigate whether the role of microbiota, not antibiotics per se, has impacts on potential muscle function, we included NAT by allowing ATB to restore microbiota through providing soiled litter from CTL after cessation of antibiotics treatment. More precisely, the NAT group received the same antibiotic mixture during the first 10 days of the experiment. Next, antibiotic mixture was removed. During the following a 10-day reseeding period, the NAT group received two times soiled litter from CTL group cages. For all groups, bottles were filled with filtered animal care drinking water. All antibiotic bottles were changed every 2 days. Feces were individually collected at *days* (D) *0*, D7, and D21. After 21 days and overnight fasting, mice were weighed and euthanized.

Euthanasia and Sampling

Mice were euthanized by intraperitoneal injection of ketamine (100 mg/kg) and xylazine (20 mg/kg). The soleus, quadriceps, extensor digitorum longus (EDL), gastrocnemius muscles, white adipose tissue, brown adipose tissue, and cecum were isolated and weighed. Muscles, intestinal sections (duodenum, jejunum, ileum, and colon), and cecum content were collected and immediately frozen in liquid nitrogen.

In Vivo Running Performance

Running performance was assessed in the three groups (CTL, ATB, and NAT) at the beginning (D0), after 1 wk of antibiotic treatment (D7–D8), and before the end of the experiment (D17–D18). Maximal aerobic velocity (MAV) was determined with a running test in which the speed was gradually increased by 2 m/min from 10 m/min until exhaustion. Exhaustion was defined as the inability to maintain the normal running position and/or after five consecutive seconds in contact with the shock grid (<0.2 mA) at the rear of the treadmill. Endurance capacity was estimated by calculating the endurance limit time (T_{lim}) during a submaximal running test, in which the speed started at 12 m/min for the first 2 min and was individually set to 70% of MAV until exhaustion. All tests were repeated at the same time of the day.

Ex Vivo Muscle Contractile Function

Muscle contractile properties were assessed in ex vivo conditions as previously described (54, 60). This technique allows evaluating the intrinsic muscle contractile properties. After 15 min equilibration in the bath, EDL samples were connected to a force transducer/length servomotor system (model 305B; Cambridge Instruments, Aurora Scientific, Ontario, Canada) and were stimulated along their entire length with platinum wire electrodes. The optimum muscle length (i.e., the muscle length producing maximal twitch tension) was determined. All subsequent measurements were made at optimum muscle length. The isometric tetanic tension was determined (701B Stimulator; Aurora Scientific) using stimulation trains of 500 ms, with pulse duration of 0.5 ms at different frequencies, from 1 to 150 Hz. Stimulus trains were separated by a 1-min interval. The maximum isometric tetanic tension (P_0) was determined from the plateau of the frequency-tension curve. After the tension-frequency determination (3 min), the resistance to fatigue was evaluated using a low-frequency fatigue protocol of 50-Hz trains of 700 ms delivered every 2 s for 5 min (43). The muscle fatigue index was defined as the time taken to produce a 50% reduction from the initial maximum power output. After all measurements, EDL samples were removed from the bath, trimmed of the connective tissue, blotted dry, and weighed.

Composition of Fecal Microbiota

DNA extraction from feces. Total cellular DNA was extracted from 0.1 g of animal fecal material using the G'NOME kit (BIO 101, La Jolla, CA) with modifications (26). Fecal samples were homogenized in the supplied cell suspension solution. Cell lysis/denaturing solution was then added, and samples were incubated at 55°C for 2 h. To improve cell lysis, 0.1-mm-diameter silica beads (750 μl) were added, and samples were mixed at maximum speed in a Beadbeater (Biospec, Bartlesville, OK) for 10 min. Polyvinylpolypyrrolidone (15 mg) was

added to ensure removal of polyphenol contamination that could inhibit the quantitative PCR (qPCR) assays. Samples were vortexed and centrifuged at 20,000 *g* for 3 min, and supernatants were recovered. The remaining pellets were washed with 400 μl of 50 mM Tris (pH 8), 20 mM EDTA (pH 8), 100 mM NaCl, and 1% polyvinylpolypyrrolidone and centrifuged at 20,000 *g* for 3 min. The washing step was repeated once more, and the resulting supernatants were pooled. Nucleic acids were precipitated by addition of 1 vol of isopropanol, incubation at −20°C for 20 min, and centrifugation at 20,000 *g* for 10 min. Pellets were resuspended in 400 μl of distilled water plus 100 μl of salt-out mixture and incubated at 4°C for 10 min. Samples were spun at maximum speed for 10 min, and DNA-containing supernatants were transferred to clean 1.5-ml microcentrifuge tubes. DNA was precipitated with two volumes of 100% ethanol at room temperature for 5 min followed by centrifugation at 16,000 *g* for 5 min. DNA was resuspended in 150 μl of Tris-EDTA buffer and stored at −20°C.

Evaluation of total bacteria by real-time qPCR analysis of bacterial 16S rRNA genes. The total bacteria present in the fecal samples of each mouse was evaluated by real-time qPCR targeting "all bacteria" 16S rRNA genes using the universal primers F-bact1369 CGGTGAATACGTTCCCGG and R-prok1492 TACGGCTACCTTGTTACGACTT (26). Analyses were performed using the StepOne Plus detection system (Applied Biosystems, Courtaboeuf, France) with 10 μl of Mastermix (PowerUpSybrGreen Master Mix; ThermoFisher Scientific, Courtaboeuf, France), 500 nM of both forward and reverse primers, and 5 μl of diluted cDNA template and water to a final volume of 15 μl. All qPCR assays were performed in duplicate using the following cycling conditions: 50°C for 2 min and then 95°C for 2 min followed by 40 cycles of 95°C for 3 s and 60°C for 30 s, with a final melting step to improve the amplification specificity. For the quantification, the *E. coli* DNA standard curve was generated by plotting the threshold cycles (C_t) versus bacterial quantity. When qPCR assays were performed using fecal DNA samples, this standard curve was used to quantify the bacterial population. The lower limit of detection for bacterial enumeration with good precision is 10^6 bacteria per gram of stool.

Evaluation of microbiota composition. The V3–V4 region of the 16S rRNA genes was amplified using the bacterial primers 343F (5′-CTT TCC CTA CAC GAC GCT CTT CCG ATC TAC GGR AGG CAG CAG-3′) and 784R (5′-GGA GTT CAG ACG TGT GCT CTT CCG ATC TTA CCA GGG TAT CTA ATC CT-3′) modified to add adaptors during the second PCR amplification. PCR assays were performed using the MolTaq 16S DNA polymerase and the corresponding master mix (Molzym, Bremen, Germany). The PCR mix contained 10 ng of DNA, 1 μl of dNTPs (10 mM), 1.25 μl each of forward and reverse primer (20 μM), and 0.5 μl of Taq polymerase in a total volume of 50 μl. The cycling program was as follows: 94°C for 3 min, followed by 40 cycles at 94°C for 15 s, 60°C for 30 s, 72°C for 60 s, and a final extension at 72°C for 5 min. Sequencing was performed using the MiSeq technology (Illumina) at the Genopole Toulouse Midi-Pyrenees (GeT) genomics facility (https://get.genotoul.fr/).

Metagenomics analysis. Sequencing data were demultiplexed at the GeT platform. The Galaxy-supported pipeline, called FROGS (Find, Rapidly, Otus with Galaxy Solution), is designed to analyze large sets of amplicon sequences and produce abundance tables of Operational Taxonomic Units (OTUs) and their taxonomic affiliation (23). Briefly, this pipeline includes a preprocessing step where reads are merged with FLASH (45), dereplicated, and filtered according to their length, mismatches in primers with cutadapt (47), and N content. This step is followed by Swarm clustering (46) with an agglomeration distance of $d = 3$. Chimera detection is then performed using Vsearch (59) before applying an OTU abundance filter (OTUs <0.005% of the total abundance are discarded; see Ref. 8). The most abundant sequences of each OTU were then affiliated with blastn against the Silva v132 database (55). Abundance tables and taxonomy files were manually imported into RStudio (v1.1.419) package Phyloseq 1.23.1 (48). Estimates of bacterial OTU diversity were estimated using the Shannon and Simpson indexes, in addition to observed richness and Chao indexes. β-Diversity analyses were performed on weighted and unweighted Jaccard and Bray-Curtis distances matrix of DNA samples and were then visualized using principal coordinate analysis and the ggplot2 R package.

Bacteriodetes and Firmicutes prevalence in ATB group. We explored the phyla levels in the ATB group despite a very low bacteria DNA concentration in these samples. We quantified two main phyla by real-time qPCR analysis using PCR primers specific for the ribosomal gene of two main bacterial phyla (Bacteroidetes and Firmicutes) gathered from the literature: Firm934F, GGAGYATGTGGTTTAATTCGAAGCA, Firm1060R, AGCTGACGACAACCATGCAC for Firmicutes (29) and mouse intestinal bacteroides forward, GGCGACCGGCGCACGGG, mouse intestinal bacteroides reverse, GRCCTTCCTCTCAGAACCC for Bacteroidetes (49).

Muscle Fiber Phenotype

The muscle fiber phenotype was determined by assessing the presence of the different myosin heavy chain (MHC) isoforms (slow MHC I and fast MHC IIa, IId/x, IIb isoforms), as previously described (20, 66). To obtain cytosolic protein extracts, gastrocnemius samples were lysed in cold lysis buffer [10 mM Tris·HCl, pH 7.4, 0.5 M sucrose, 50 mM NaCl, 5 mM EDTA, 30 mM $Na_4P_2O_7$, 1% Nonidet P-40, 0.25% sodium deoxycholate, 50 mM NaF, 100 μM sodium orthovanadate, and proteases inhibitor cocktail (5 μl/ml, P8340; Sigma)]. Protein concentration was determined using the Lowry assay. Protein samples (6 μg) were separated on high-glycerol-containing (30%) gels with an acrylamide-to-bis-acrylamide ratio of 50:1 for the separating gel (8% total acrylamide, pH 8.8) and for the stacking gel (4% total acrylamide, pH 6.8) using a Mini-Protean II dual-slab cell apparatus (Bio-Rad, Hercules, CA). After electrophoresis (at 140 V in a refrigerated room at 4°C for 22 h), gels were stained with Coomassie blue (IRDye Blue Protein Stain; LI-COR Biosciences, Lincoln, NE), and the different MHC isoforms were identified according to their electrophoretic mobility pattern (20, 66).

Cross-Sectional Muscle Fiber by Immunohistochemistry

Serial transverse sections (10 μm thick) from liquid nitrogen-cooled isopentane frozen quadriceps muscle samples were obtained using a cryostat at −25°C and mounted on glass microscope slides. Sections were then washed in phosphate-buffered saline (PBS), blocked, and permeabilized with 0.1% Triton X-100 and 10% horse serum. For fiber cross-sectional area (CSA) determination, sections were stained with an anti-laminin antibody (1:200 in PBS, L9393; Sigma) at 37°C for 1 h, followed by washes in PBS and incubation with the secondary antibody Alexa Fluor 488 goat anti-rabbit IgG (1:1,000 in PBS, A11034; Invitrogen) for 1 h. Whole histological sections were imaged with a digital slide scanner Hamamatsu NanoZoomer 2.0-HT and analyzed with the ImageJ software package. On average, 1,800 fibers/animal were quantified according to the method of Demangel et al. (19).

Transcript and Protein Expression Profiles in Ileum and Skeletal Muscle

To explore potential mechanisms linking gut microbiota composition and skeletal muscle, we measured markers involved in protein turnover, mitochondrial metabolism (36), inflammation, and related to lipid and glucose metabolism in both ileum and/or muscle, as described below (Tables 1 and 2).

Immunoblotting. Frozen gastrocnemius muscle samples were homogenized using an Ultra-Turrax homogenizer in an ice-cold extraction buffer (20 mM Tris, pH 7.4, 150 mM NaCl, 1 mM EDTA, 0.1% SDS, and 1% Triton X-100) with 0.5% protease inhibitors, 1% Nonidet P-40, 0.25% sodium deoxycholate, 0.2% NaF, and 100 μM

Table 1. *List of primary antibodies used for Western Blotting*

Marker	Protein	Molecular Weight, kDa	Reference	Source	Dilution
Protein turnover	4EBP1	17	Cell Signaling, 9644	Rabbit	1:1,000
	p-4EBP1$^{Thr37/46}$	17	Cell Signaling, 2855	Rabbit	1:1,000
	RPS6	32	Cell Signaling, 3944	Rabbit	1:1,000
	p-RPS6$^{Ser235/236}$	32	Cell Signaling, 4856	Rabbit	1:1,000
	PRAS40	40	Cell Signaling, 2691S	Rabbit	1:1,000
	p-PRAS40^{T246}	40	Cell Signaling, 13175S	Rabbit	1:1,000
	LC3b	14	Cell Signaling, 3868	Rabbit	1:1,000
Energetic Sensor	AMPKα	62	Cell Signaling, 5832	Rabbit	1:1,000
	p-AMPKα^{THR172}	62	Cell Signaling, 2535	Rabbit	1:1,000
Mitochondrial metabolism	PGC1-α	105	Calbiochem, 516557	Rabbit	1:1,000
	COX IV	17	Santa Cruz, sc-69360	Mouse	1:200

AMPKα, AMP-activated protein kinase-α; PGC-1α, peroxisome proliferator-activated receptor coactivator-1α; COX IV, cyclooxygenase IV; 4EBP1, eukaryotic translation initiation factor 4E-binding protein 1; RPS6, ribosomal protein S6PRAS40, proline-rich Akt substrate of 40 kDa; LC3b, microtubule-associated protein light chain 3b.

sodium orthovanadate added just before extraction. Samples containing 50 μg of proteins were resolved on 10–15% SDS-PAGE and transferred to a nitrocellulose membrane. Total proteins were visualized by Ponceau red staining to verify equal loading. Blots were blocked with 5% bovine serum albumin (BSA) in TBS-0.2% Tween 20 (TBST) for 1 h, followed by overnight incubation with antibodies against proteins involved in muscle metabolism and proteolysis/synthesis balance (Table 1). After three 5-min washes at room temperature with TBST, membranes were incubated with a secondary antibody conjugated with horseradish peroxidase at room temperature for 1 h. Blots were washed (three times for 5 min each) with TBST at room temperature, and antibody-bound proteins were revealed using the ECL reagent (Bio-Rad Life Science). Films were scanned and analyzed using the Image Laboratory software. All blots were corrected for loading based on the Ponceau red staining.

RNA isolation and RT-qPCR. Total RNA was isolated from gastrocnemius and ileum samples using TRIzol Reagent (200 ml, 15596–018; Invitrogen). RNA concentration was determined by spectrophotometry (Eppendorf, Hamburg, Germany), and purity was checked by calculating the ratio of optial dencity at 260 to 280 nm (>1.7). RNA quality was verified by 1% agarose gel electrophoresis. Reverse transcription was performed with 1 μg of total RNA and the TAKARA kit (TAKRR037A, PrimeScript RT reagent Kit, Perfect Real Time) according to the manufacturer's instructions. qPCR analysis was performed using the StepOnePlus Real-Time PCR System (Applied Biosystems) with 10 μl of Powerup SYBR Green Master Mix (A25742; ThermoFisher Scientific), 10 nM of both forward and reverse primers (Table 2), and 5 μl of diluted cDNA (final volume of 15 μl). All PCR assays were performed in duplicate using the following cycling conditions: 50°C for 2 min and then 95°C

Table 2. *Gene expression in skeletal muscle and ileum: sequences of primers (5′–3′)*

Markers	Gene	Reference	Forward	Reverse
			Gene expression in skeletal muscle	
Protein turnover	*Igf-1*	XM_006513261.2	AGCAGCCTTCCAACTCAATTAT	GAAGACGACATGATGTGTATCTTTATC
	FoxO3a	XM_006512806.1	GGAAATGGGCAAAGCAGA	AAACGGATCACTGTCCACTTG
	Murf1 (Trim63)	NM_001039048.2	TCCTGCAGAGTGACCAAGG	GGCGTAGAGGGTGTCAAAC
Inflammation	*Trif (Ticam1)*	NM_174989.4	CAGCTCAAGACCCCTACAGC	CTCCCACACAGCCTCGTC
	Nf-κB	NM_008689.2	TGAGGACGGGGTATGCAC	TCACATGAAGTATTCCCAGGTTT
Lipid transport	*CD36*	NM_001159557.1	CAGATCCGAACACAGCGTAG	GCGACATGATTAATGGCACA
Mitochondrial metabolism	*Cpt1*	NM_009948.2	CATCCCAGGCAAAGAGACA	AAGCGACCTTTGTGGTAGACA
	Nrf-1	NM_001164226	GGTGGGGGACAGATAGTAGTCT	ATGCTCACAGGGATCTGGAC
Mitochondrial content	*ATP5b*	NC_000076	GTTTGCTGAAGCCACACTCA	CATGATTCTGCCCAAGGTCT
	ND2	NC_005089.1	AAGGGATCCCACTGCACATA	AGTCCTCCTCATGCCCCTAT
	ND5	NC_005089.1	ATAACCGCATCGGAGACATC	GAGGCCAAATTGTGCTGATT
			Gene expression in ileum	
Glucose and lipid metabolism	*Fiaf (Angptl4)*	NM_020581.2	GGGACCTTAACTGTGCCAAG	GAATGGCTACAGGTACCAAACC
Inflammation	*Myd88*	NM_010851.2	GCCTTGTTAGACCGTGAGGAT	CTAAGTATTTCTGGCAGTCCTCCT
	Tlr4	NM_021297.3	GGACTCTGATCATGGCACTG	CTGATCCATGCATTGGTAGGT
Branched amino acids receptor	*Lat-1*	NM_011404.3	ATGTGGCTCCGATTCAAGA	GGAGGGCCAGATTCACCT
Short-chain fatty acid receptor	*Gpr40 (Ffar1)*	NM_194057.2	AGGCGCTCTCCTCACACTC	CTAGCCACATTGGAGGCATTA
Mean-chain fatty acid receptor	*Gpr41 (Ffar3)*	NM_001168509.1	TGCTCTGAAGAAGCCAATCA	TTCTCCTCTGGTCCAGTGCT
Long-chain fatty acid receptor	*Gpr120 (Ffar4)*	NM_181748.2	TTGGTGTTGAGCGTCGTG	CCAGCAGTGAGACGACAAAG
Glucose transporter	*Sglt1*	NC_000071.6	CTGGCAGGCCGAAGTATG	TTCCAATGTTACTGGCAAAGAG
Reference gene	*Arp (Rplp0)*	NM_007475.5	ACTGGTCTAGGACCCGAGAAG	TCCCACCTTGTCTCCAGTCT
	α-Tubulin	NM_011653.2	CTGGAACCCACGGTCATC	GTGGCCACGAGCATAGTTATT

Igf, 1, insulin-like growth factor-I; Foxo3a, forkhead box O3; Murf1, muscle RING-finger protein-1; Trif, TIR-domain-containing adapter-inducing interferon-β; CD36, cluster of differentiation 36; Cpt1, carnitine palmitoyltransferase 1; Nrf1, nuclear respiratory factor 1; ATP5b, ATP synthase F1 subunit β; ND2, mitochondrially encoded NADH dehydrogenase 2; ND5, mitochondrially encoded NADH dehydrogenase 5; Fiaf, fasting-induced adipose factor; Myd88, myeloid differentiation primary response 88; Tlr4, Toll-like receptor 4; Lat-1, large neutral amino acid transporter 1; Gpr40, G protein-coupled receptor 40; Gpr41, G protein-coupled receptor 41; Gpr120, G protein-coupled receptor 120; sodium/glucose cotransporter 1; Sglt1, sodium-glucose cotransporter 1; Arp, acidic ribosomal phosphoprotein.

for 2 min followed by 40 cycles of 95°C for 3 s and 60°C for 30 s. The relative mRNA levels were normalized to α-tubulin (α-tub) and acidic ribosomal phosphoprotein P_0, as housekeeping genes unaffected by the experimental conditions. Results were expressed using the C_t method to generate $\Delta\Delta C_t$ values with template dilutions ranging from 10^1 to 10^6 copies. The PCR overall efficiency (E) was calculated from the slopes of the standard curves according to the equation $E = [10^{(-1/slope)}] - 1$, and this value was higher than 95% for all assays. The relative abundance of each sample was then normalized according to the equation: relative quantity $= 2^{-\Delta\Delta C_T}$. All of the experiments were performed according to the minimum information for publication of quantitative real-time PCR experiment (MIQE) guidelines (11, 61).

Mitochondrial DNA isolation and measurement by RT-qPCR. Total DNA was extracted from the gastrocnemius muscle using a QIAamp DNA kit (Qiagen). Genomic (ATP synthase-β) and mitochondrial DNA (means of NADH dehydrogenase subunit 5 and NADH dehydrogenase subunit 2) were quantified by quantitative real-time polymerase chain reaction (10). Each sample was run in duplicate. Results were expressed using the C_t with genomic DNA as the control. The relative changes in the expression level of mitochondrial DNA were calculated by the $\Delta\Delta C_t$ formula.

Muscle Glycogen Content

The acid-hydrolysis method used for glycogen quantification was adapted from the protocols described by Adamo and Graham (1) and Jansson (38). Frozen gastrocnemius muscle powder (20–30 mg) was placed in ice-cooled 6% perchloric acid and 1 M hydrochloric acid. Samples were then boiled at 100°C for 2 h, cooled on ice for 10 min, and centrifuged (1,300 revolutions/min for 5 min). Supernatant (12 μl) was removed from each sample, diluted in 200 μl of GOD-PAP solution (Biolabo, Maizy, France), and incubated in the dark at 37°C for 20 min to determine the glucose concentration. Absorbance was measured at 500 nm using a microplate reader. Glycosyl units produced by glycogen hydrolysis were expressed as micromole per milligram of wet muscle weight.

Muscle Triglyceride Content

Muscle triglycerides were determined by using the DiaSys kit (Diagnostic System, Grabels, France) following a preliminary organic phase extraction according to Bligh & Dyer's method. Briefly, 50 μg of gastrocnemius samples were crushed with 500 μl of 150 mM sodium chloride. Next, 150 μl of muscle homogenates were extracted with 600 μl of a methanol-chloroform mixture (1:1, vol/vol). The organic layers were collected after centrifugation (10,000 *g* for 10 min) and dried under nitrogen. Dry samples were reconstituted in 37.5 μl of isopropanol-acetonitrile-water mixture (2:1:1, vol/vol/vol), and 10 μl were analyzed according to the manufacturer's recommendations (7).

Statistical Analysis

All data are presented as means ± SE. The normality of each distribution and homogeneity of variance were assessed with the Kolmogorov-Smirnov and Fischer test, respectively. Significance between CTL, ATB, and NAT data was checked using a one-way analysis of variance. Significant interaction effects were analyzed with the Fischer least-significant difference post hoc test. For some parameters, the unpaired *t*-test was used to compare directly CTL versus NAT or CTL versus ATB. The Mann-Whitney rank-sum test was chosen when the normality and/or equal-variance tests failed. For running tests, significance between parameters at D0, D7, and D17 was checked using the paired *t*-test, after checking normality. For all statistical analyses, the significance level was set at 0.05. Data were analyzed using the statistical package GraphPad Prism version 6.02 for Windows (GraphPad Software, La Jolla, CA).

Table 3. *Effects of antibiotic treatment and natural reseeding on body mass, glycemia, cecum liver and adipose tissue weights, as well food intake and hydration*

	CTL	ATB	NAT
Body wt, g	25.5 ± 0.8	25.4 ± 0.4	25.0 ± 0.7
Glycemia, mg/dl	101.0 ± 3.8	101.7 ± 5.1	93.4 ± 4.4
Cecum wt, mg	324.7 ± 35.0	1,804.0 ± 154.0***	394.9 ± 25.2†††
Liver wt, mg/g	44.3 ± 1.4	38.3 ± 0.7**	42.3 ± 1.2††
Adipose tissue wt, mg/g			
White adipose tissue	27.8 ± 4.4	19.8 ± 3.2	26.4 ± 2.1
Brown adipose tissue	3.0 ± 0.2	2.7 ± 1.7	3.4 ± 0.2
Food intake, g/wk	29.9 ± 1.2	28.4 ± 1.1	29.0 ± 0.7
Hydration, ml/wk	34.6 ± 1.9	36.1 ± 1.6	36.0 ± 1.1

Values are group means at *day 21* for weights and weekly for food intake and hydration ± SE; $n = 9$–10 for each group. CTL, control; ATB, group treated with antibiotics for 21 days; NAT, treated with antibiotics for 10 days followed by natural reseeding for another 11 days; *Rplp0*, ribosomal phosphoprotein P_0. Significance was checked using ANOVA followed by least-significant difference Fisher post hoc test. $^{**}P \leq 0.01$ and $^{***}P < 0.001$ versus the CTL group. $^{††}P < 0.01$ and $^{†††}P < 0.001$ versus the ATB group.

RESULTS

Treatment Tolerance

During the entire study period, neither diarrhea nor visible adverse side effects were recorded. Consequently, no mouse was excluded from the data analysis. Food intake and hydration were checked daily, and no significant change was observed during the entire study period (Table 3).

Antibiotic Treatment and Natural Reseeding Efficiently Modulate Gut Microbiota

To confirm gut microbiota depletion induced by the antibiotic treatment, we quantified by Q-PCR all bacteria in feces, as well as cecum weight (cecum hypertrophy is a marker of gut microbiota depletion; see Ref. 56). At D0, microbiota DNA content did not differ in the three mouse groups (CTL, ATB, and NAT) (Fig. 1*A*). After 7 days of antibiotic treatment (D7), bacterial DNA content was strongly reduced in the ATB and NAT groups (Fig. 1*B*). This effect was still present in the ATB group after 21 days of treatment (D21) (Fig. 1*C*). Despite a very low bacteria DNA concentration in gut samples in the ATB group at D21, we managed to estimate the phyla prevalence by qPCR analysis and found the following: 83% of Firmicutes and 17% of Bacteriodetes; the other phyla were not detectable (data not shown).

Conversely, natural reseeding restored the bacterial DNA level in the NAT group (Fig. 1*C*). At D21, α-diversity (Fig. 1*D*) and β-diversity analyses (Fig. 1, *E* and *F*) showed no statistical differences in microbiota between CTL and NAT groups. Neither phyla abundance (Fig. 1, *G* and *H*) nor levels of the main family from Bacteroides and Firmicutes showed statistical differences between CTL and NAT groups (Fig. 1, *I* and *J*). Moreover, cecum weight at D21 was significantly higher in ATB mice than in the CTL group (+456%, $P < 0.001$; Table 3). Cecum weight in the NAT group was significantly lower than in the ATB group (−76%, $P = 0.003$) and did not significantly differ from that

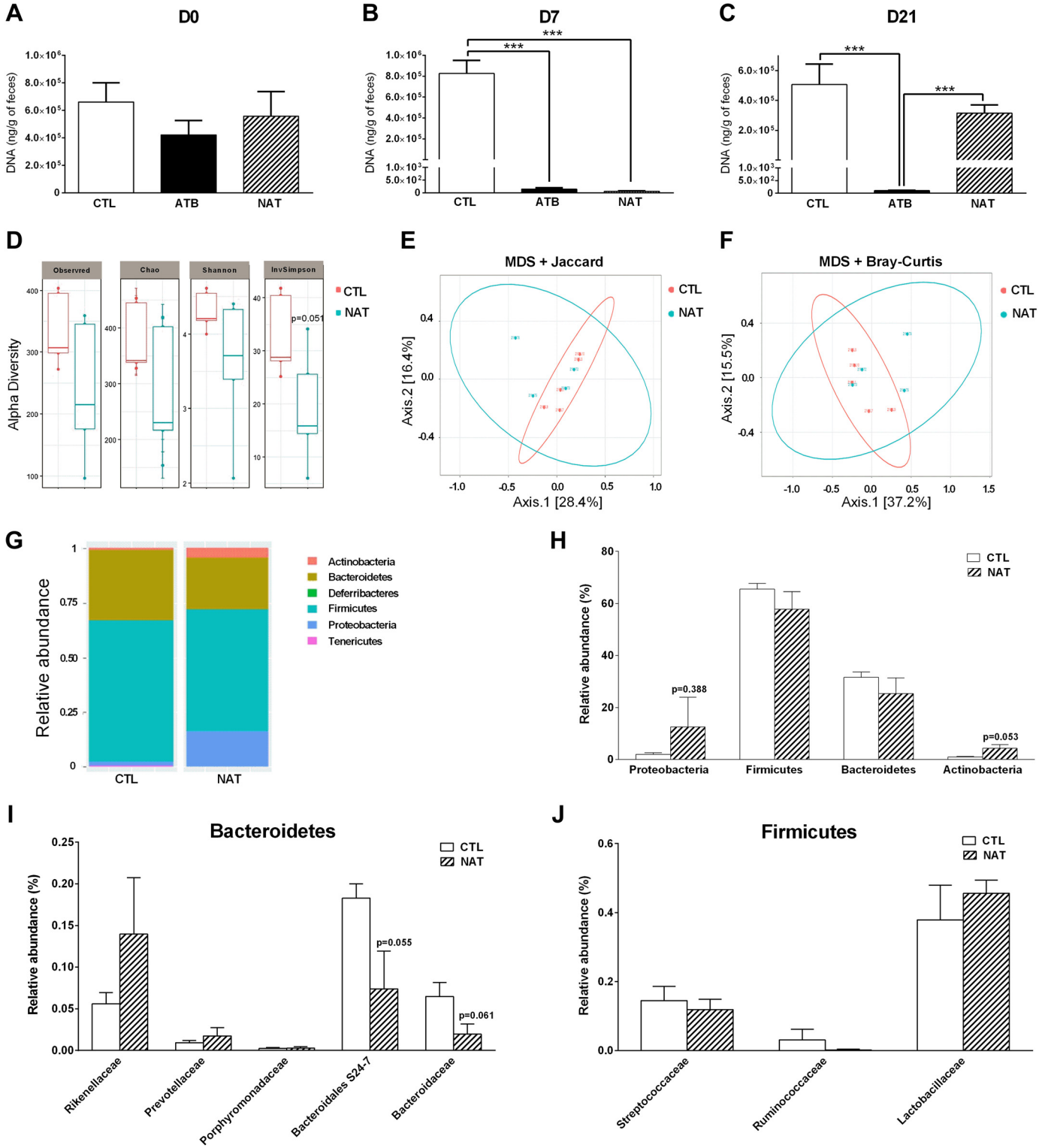

Fig. 1. Effect of gut microbiota depletion and natural reseeding on bacterial DNA content, α- and β-diversity indexes, and phyla and families abundance. Real-time quantitative PCR (qPCR) quantification of all bacteria in feces at *day* (D) *0* (*A*) and D7 (*B*) and in the cecum at D21 (*C*) ($n = 5$). Bacterial α-diversity (*D*) and β-diversity (*E* and *F*) in cecum at D21 ($n = 5$). Sample denotation: red, control (CTL); blue, treatment with antibiotics for 10 days followed by natural reseeding for another 11 days (NAT). Bacterial phyla (*G* and *H*) and families (*I* and *J*) abundance in cecum at D21 ($n = 5$). For bacterial DNA content, a 1-way ANOVA followed by the least-significant difference (LSD) Fisher post hoc test was used. To evaluate the reseeding process, bacterial and families abundance, as well as α-diversity, was compared in CTL and NAT groups using unpaired nonparametric *t*-test. For β-diversity, significance between CTL and the group treated with antibiotics for 21 days (ATB) was checked using PERMANOVA, as implemented in the "Adonis" function from the R vegan package, with 9,999 permutations. ***$P \leq 0.001$ vs. CTL, ATB, and NAT.

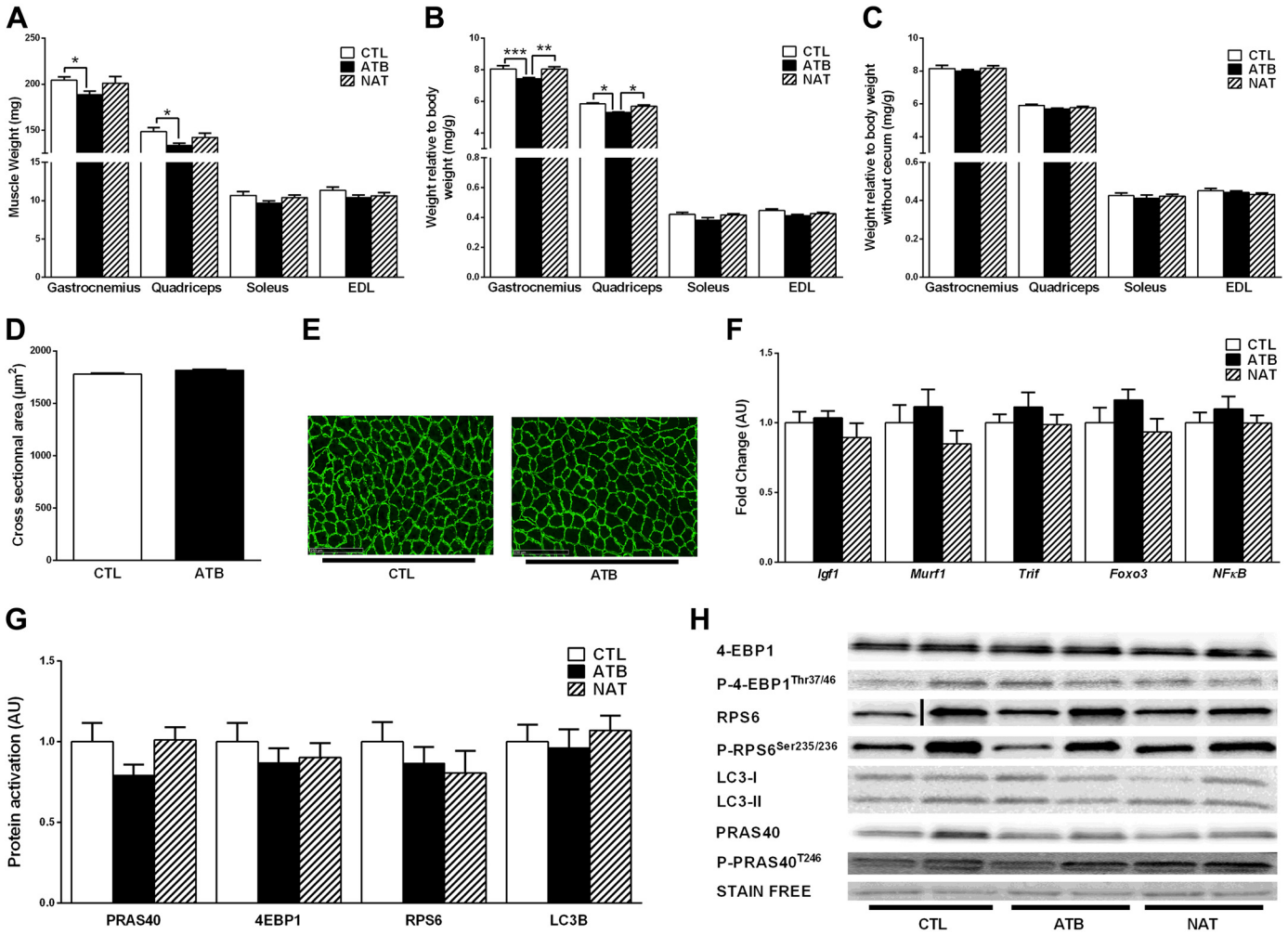

Fig. 2. Effects of gut microbiota depletion and natural reseeding on skeletal muscle structure. Wet weight (*A*) and weight relative to body weight (*B*) at *day* (D) *21* in the control (CTL) group, the group treated with antibiotics for 21 days (ATB), and/or mice treated with antibiotics for 10 days followed by natural reseeding for another 11 days (NAT) in the gastrocnemius, quadriceps, soleus, and extensor digitorum longus (EDL). *C*: weight relative to body weight after subtraction of cecum weight at D21. *D*: quadriceps fiber cross-sectional area (CSA) distribution at D21. *E*: representative images of quadriceps muscle sections at D21. *F*: RT-quantitative PCR (qPCR) analysis of *Igf-1*, *Murf-1*, *Trif*, *Foxo-3a*, and *Nf-κB* expression in gastrocnemius muscle at D21. *G*: activation of PRAS40, 4EBP1, RPS6, and LC3B in gastrocnemius muscle at D21. *H*: representative blotting images used for the quantification shown in *G*. On the blot for RPS6 (*G*), a line was added to show an arrangement because of an empty well between the samples on the Western blot gel. Values are means ± SE. Significance between CTL, ATB, and NAT was checked using a 1-way ANOVA followed by the least-significant difference (LSD) Fisher post hoc. The mean muscle fiber CSA was compared in CTL and NAT groups using unpaired *t*-test (*D*). $*P \leq 0.05$, $**P \leq 0.01$, and $***P \leq 0.001$ ($n = 8$–10 for each group).

of the CTL group (Table 3). All together, these results support that the NAT group can be used to assess the effects of gut microbiota per se on skeletal muscle function together with the ATB group.

Effects of Gut Microbiota Depletion on the Structure of Skeletal Muscle Mass

At the end of the study, the muscle wet weight (Fig. 2*A*) and mass index calculated as wet weight normalized to the whole body weight (Fig. 2*B*) were significantly lower for gastrocnemius and quadriceps, but not for EDL and soleus, in the ATB group compared with the CTL and NAT groups (on average, between 7 and 10% of reduction). Normalization to the whole body weight could be misleading because of the cecum hypertrophy in the ATB group (Table 3). Indeed, when the muscle mass index was normalized to body weight without the cecum weight, the weight of gastrocnemius, quadriceps, EDL, and soleus was comparable between CTL and ATB mice (Fig. 2*C*). Moreover, histological analysis on quadriceps muscle samples showed that the fiber CSA was comparable between CTL and ATB groups (Fig. 2, *D* and *E*). Similarly, gene/protein activation of several key factors involved in protein synthesis, proteolysis, inflammation, and autophagy (*Igf1*, *Murf1*, *Trif, Foxo-3a*, and *NfκB*, PRAS40, 4EBP1, RPS6, and LC3B) was comparable in the gastrocnemius muscle of CTL and ATB mice (Fig. 2, *F–H*).

Gut Microbiota Depletion Induces Muscle Fatigability That Is Reversed by Natural Reseeding

To determine the impact of gut microbiota depletion/natural reseeding on skeletal muscle function, mice under-

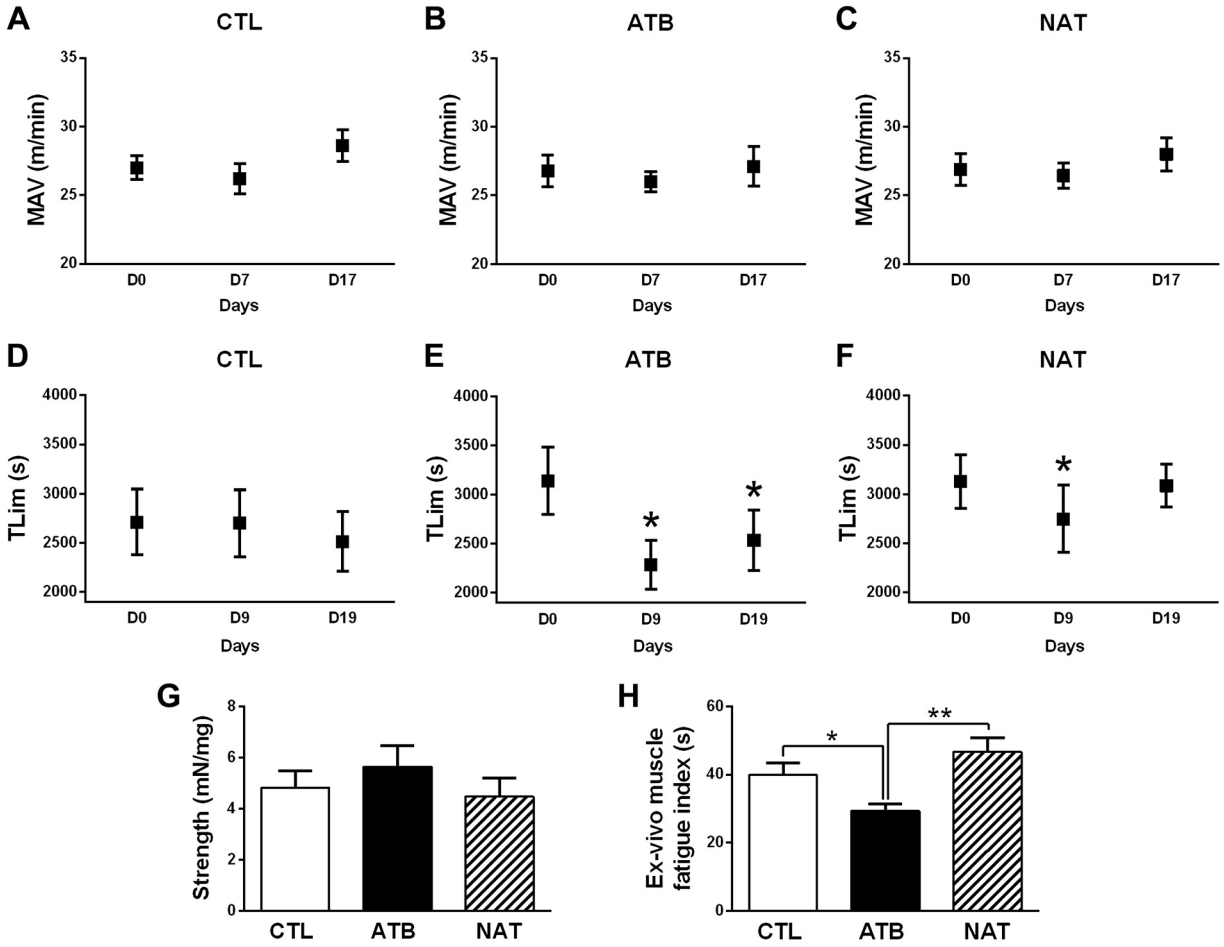

Fig. 3. Effects of gut microbiota depletion and natural reseeding on skeletal muscle function. Maximal aerobic velocity (MAV) in the control group (CTL, *A*), the group treated with antibiotics for 21 days (ATB, *B*), and the group treated with antibiotics for 10 days followed by natural reseeding for another 11 days (NAT, *C*) at *day* (D) *0*, D7, and D17. Limit time to exhaustion during a submaximal running test in the CTL (*D*), ATB (*E*), and NAT (*F*) groups at D0, D9, and D19. *G*: ex vivo extensor digitum longus (EDL) maximal strength relative to its weight at D21. *H*: ex vivo EDL muscle fatigue index at D21. Values are means ± SE. Significance was checked using the paired *t*-test (*A–F*) and a 1-way ANOVA followed by the least-significant difference (LSD) Fischer post hoc test (*G* and *H*). $^{*}P \leq 0.05$ vs. D0 (*E* and *F*) and ATB vs. CTL (*H*). $^{**}P \leq 0.01$, ATB vs. NAT (*H*) (n = 9–10 for each group).

went running tests at different time points. Moreover, at the end of the study, we tested ex vivo the contractile properties of EDL muscle samples to identify the specific role of skeletal muscle on the running performance (Fig. 3). MAV, which is dependent on the maximal oxygen consumption, was comparable in the three groups (CTL, ATB, and NAT) and at all time points (D0, D7, and D17) (Fig. 3, *A–C*). Conversely, performance indicators related to endurance were significantly affected by gut microbiota changes (Fig. 3, *D–F*). Specifically, T_{lim} during the running endurance test was significantly lower at D9 compared with the D0 values in ATB and NAT mice (−27% in the ATB group, P = 0.015, and −12% in the NAT group, P = 0.012; Fig. 3*E*). At D19, T_{lim} was still lower than at D0 in the ATB group (−19.3%, P = 0.037), whereas it was back to the D0 values in the NAT group (Fig. 3*F*). Ex vivo contractile tests performed at the end of the protocol showed that EDL maximal strength was not affected by the experimental conditions (Fig. 3*G*), whereas EDL muscle fatigue index was significantly reduced in the ATB group compared with both CTL and NAT groups (−26%, P = 0.036, and −37%, P = 0.001, respectively; Fig. 3*H*). EDL muscle fatigue index in the CTL and NAT groups did not differ significantly.

Potential Mechanisms Linking Gut Microbiota and Skeletal Muscle Function: Focus on Glucose Homeostasis

Several cellular adaptations, including muscle fiber phenotype, mitochondrial biogenesis, and/or substrate availability, affect skeletal muscle endurance (22). Here, we observed that the expression of the different MHC isoforms in gastrocnemius muscle was comparable in CTL and ATB (Fig. 4, *A* and *B*). Similarly, the protein level of key markers of mitochondrial metabolism [AMP-activated protein kinase (AMPK), peroxisome proliferator-activated receptor coactivator-1α, and cyclooxygenase IV; Fig. 4, *C* and *D*] or the mRNA expression of Glut4, cluster of differentiation 36 (*Cd36*), carnitine palmitoyltransferase 1 (*Cpt1*), as well nuclear respiratory factor-1 and the mitochondrial DNA content (Fig. 4, *E* and *F*) did not change after ATB treatment. These results suggest that disruption of gut microbiota composition does not impact the myofiber phenotype or the mitochondrial metabolism.

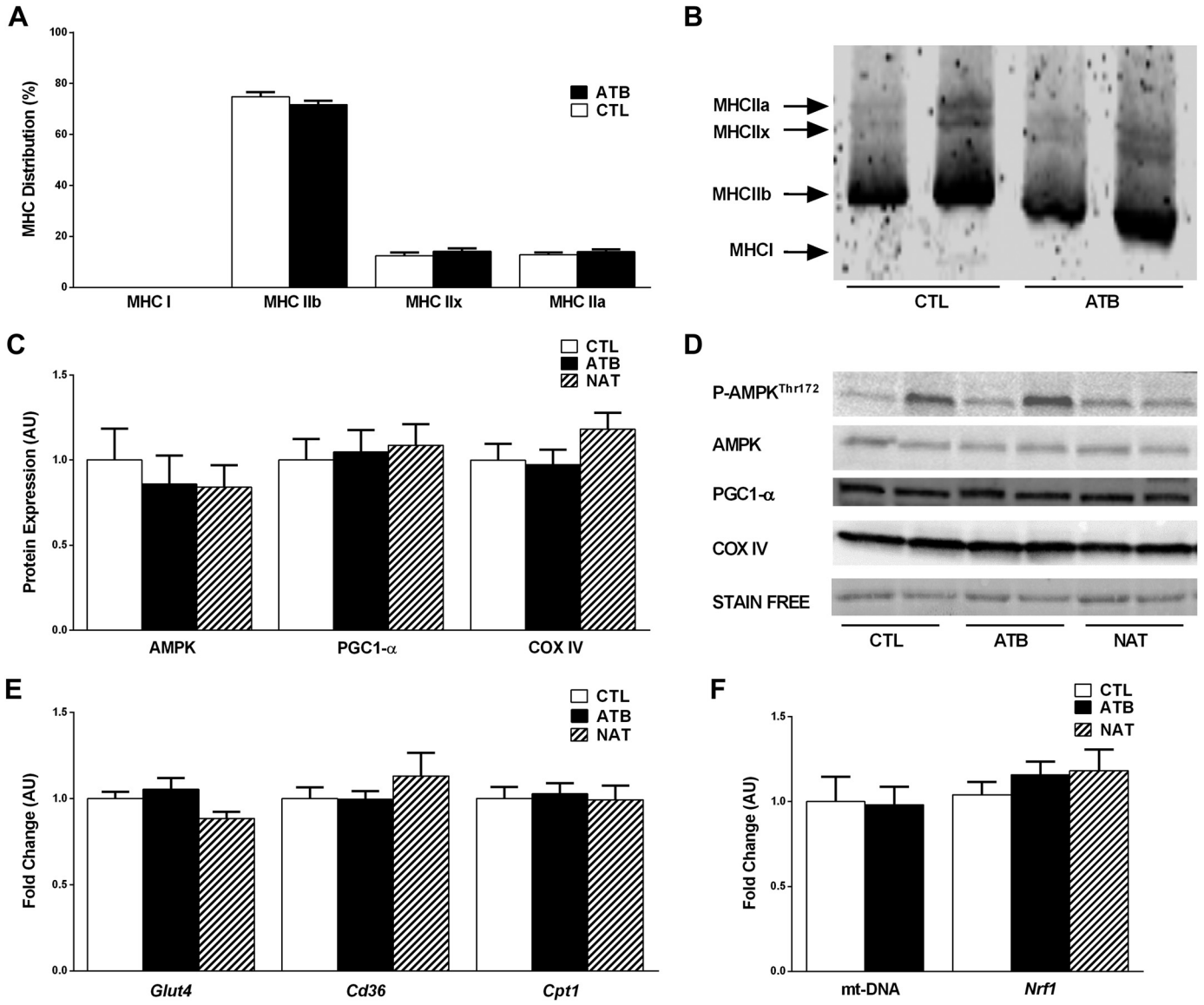

Fig. 4. Effects of gut microbiota depletion and natural reseeding on skeletal muscle metabolism. *A*: gastrocnemius myosin heavy chain (MHC) distribution at *day* (D) *21*. *B*: representative images of protein electrophoresis shown in *A*. *C*: *cluster of differentiation 36* (*Cd36*) and *carnitine palmitoyltransferase 1* (*Cpt1*) mRNA expression in gastrocnemius samples at D21. *D*: mitochondrial DNA content and *nuclear respiratory factor 1* (*Nrf-1*) mRNA expression in gastrocnemius samples at D21. *E*: AMP-activated protein kinase (AMPK) phosphorylation, peroxisome proliferator-activated receptor coactivator (PGC)-1α, and cyclooxygenase (COX) IV protein content in gastrocnemius muscles at D21. *F*: representative blotting images used for the quantification shown in *E*. Values are means ± SE. Significance between groups was checked using a 1-way ANOVA followed by the least-significant difference (LSD) Fisher post hoc test, except for mitochondrial DNA, where Mann-Whitney was used to compare CTL and the group treated with antibiotics for 21 days (ATB) (n = 8–10 for each group).

Gut microbiota depletion leads to major changes in intestinal epithelial cells (71), and the gut microbiome has a profound influence on inflammatory states (65). Here, we reported in ileum that ATB treatment and subsequent natural reseeding did not affect gene expression of myeloid differentiation primary response 88 and Toll-like receptor 4 (*Tlr4*), two canonical proteins involved in inflammatory signaling pathways (Fig. 5*A*).

As shown by others, the lack of some bacteria-derived metabolites could interfere with the metabolism of energetic substrate, such as lipid and glucose metabolism (12, 33), and this could play important roles in the gut-skeletal muscle axis. In this context, fasting-induced adipocyte factor (*Fiaf*), also known as angiopoietin like protein 4, is a key protein reducing fatty acids synthesis, adipogenesis, and lipogenesis (13). *Fiaf* expression is known to be negatively regulated by intestinal bacteria (2). In our study, *Fiaf* gene expression in ileum was indeed significantly higher in the ATB group compared with CTL and NAT groups (+164%, $P = 0.001$, and +135%, $P = 0.002$, respectively; Fig. 5*A*). However, this *Fiaf* increase was not associated with changes in muscle triglyceride levels in all experimental conditions (Fig. 5*C*). Finally, gut microbiota modulation did not affect *Lat1* expression, suggesting no major effects on branched amino acid transport (Fig. 5*A*).

Antibiotic treatment and reseeding did not exert any effect on free fatty acid receptor 1 and 4 (*Gpr40* and *Gpr120*, respectively), both receptors being activated by medium- to

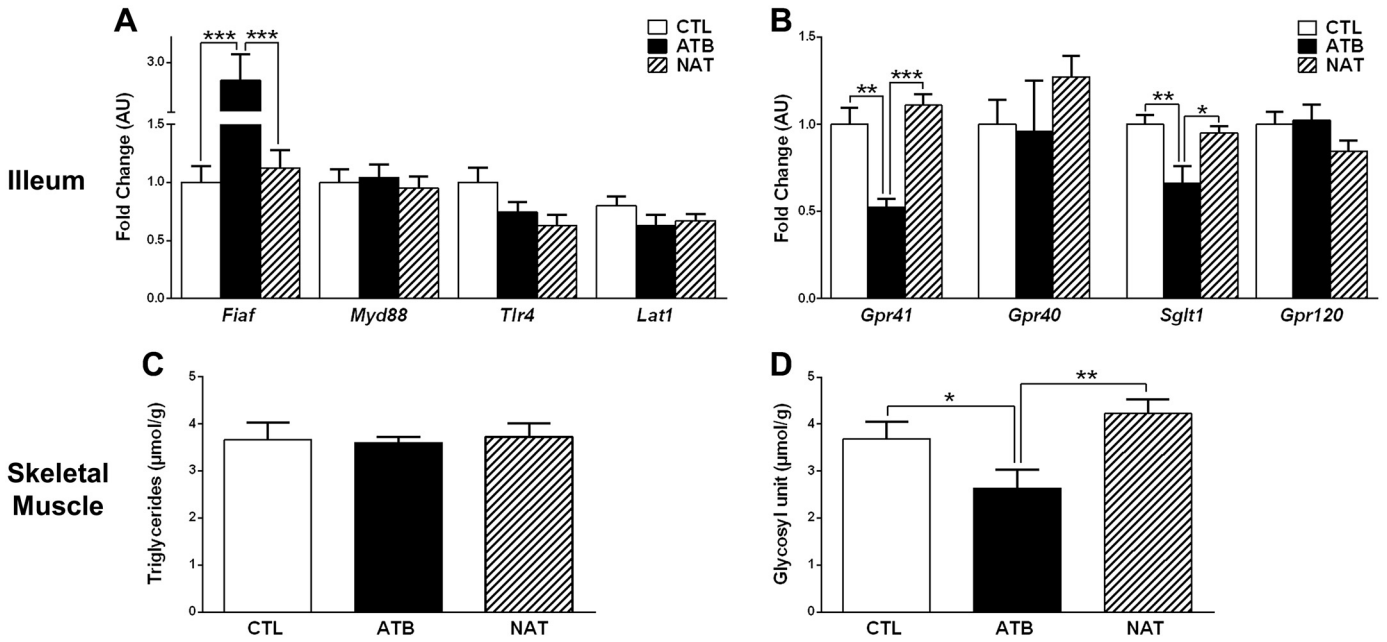

Fig. 5. Effects of gut microbiota depletion and natural reseeding on energetic substrate metabolism. *A*: RT-quantitative PCR (qPCR) expression of *Fiaf*, myeloid differentiation primary response 88 (*Myd88*), Toll-like receptor 4 (*Tlr4*), and *Lat1* in the ileum at *day* (D) *21* ($n = 8$). *B*: RT-qPCR expression of *G protein-coupled receptor* (*Gpr*) *41*, *Gpr40*, *Gpr120*, and sodium/glucose cotransporter 1 (*Sglt1*) in the ileum at D21 ($n = 8$). *C*: gastrocnemius triglyceride content at D21 ($n = 9$–10). *D*: gastrocnemius glycogen content at D21 ($n = 9$–10). Values are means ± SE. Significance between the 3 groups was checked using a 1-way ANOVA followed by the least-significant difference (LSD) Fisher post hoc test. *$P \leq 0.05$, group treated with antibiotics for 21 days (ATB) vs. CTL and group treated with antibiotics for 10 days followed by natural reseeding for another 11 days (NAT). **$P \leq 0.01$, ATB vs. CTL and NAT; ***$P \leq 0.001$, ATB vs. CTL and NAT.

long-chain fatty acids. However, short-chain fatty acids (SCFAs) are the most abundant microbial metabolites derived from intestine, and SCFAs activated enteroendocrine cells via the free fatty acid receptor 3 (*Gpr41*). Interestingly, we reported in ileum samples that *Gpr41* gene expression was significantly decreased in the ATB group compared with the CTL group (−48%, $P = 0{,}007$; Fig. 5*B*). After natural reseeding, the NAT group exhibited higher *Gpr41* mRNA levels compared with the ATB group (+111%, $P < 0.001$; Fig. 5*B*). Because the activity of these enteroendocrine receptors is linked to glucose metabolism (30, 44, 68), we measured additional markers both in ileum and skeletal muscle. It is noteworthy that the gene expression of *Sglt1* followed the same pattern in ileum as *Gpr41*, i.e., significant lower levels in the ATB condition (−34%; $P = 0.001$ versus the CTL group; Fig. 5*B*), with such effect being reversed by natural reseeding (+44%, $P = 0.033$ versus the ATB group; Fig. 5*B*). However, these gene expression changes were not associated with modification in blood glucose levels (Table 3). Finally, because glucose stored in glycogen is the one main substrate involved in muscle energy supply during endurance exercise (22), we monitored muscle glycogen content. In agreement with results obtained in ileum on *Gpr41* and *Sglt1*, muscle glycogen content was significantly lower in ATB than in CTL mice (Fig. 5*D*), and this was normalized after natural reseeding (Fig. 5*D*).

DISCUSSION

The present study is the first one designed to explore the consequences of gut microbiota depletion and reseeding on skeletal muscle structure and metabolism. Using an experimental model of gut microbiota modulation, we demonstrated negative impacts on skeletal muscle endurance, reversed by bacterial reseeding. Our ex vivo functional analyses clearly support a role of gut microbiota on muscle intrinsic contractile properties. Gut microbiota appears to play a role in glucose homeostasis, since we observed that short fatty acid chain and glucose transporters (*Gpr41*, *Sglt1*) in ileum and muscle glycogen content paralleled the muscle endurance changes observed after ATB treatment and reseeding. Altogether, our results highlight that gut microbiota depletion impact on muscle endurance can be mediated through the modulation of muscle glycogen availability.

Gut Microbiota and Muscle Mass

Research from Bindels et al. suggested a link between gut microbiota profile and skeletal muscle mass in pathological conditions (4, 6). Recently, Varian et al. (69) showed that probiotic supplementation partially prevents skeletal muscle atrophy related to cancer cachexia and sarcopenia. Here, in healthy mice, we found lower wet weight and mass index of some muscles in ATB mice. However, the cecum hypertrophy, a widely known phenomenon associated with depleted bacteria condition (41), could mask a body weight reduction in these mice, as indicated by the absence of difference on muscle mass when normalization was done after subtraction of the cecum weight. This suggests that gut microbiota modulation does not directly cause skeletal muscle atrophy in our experimental conditions. This is emphasized by the absence of changes in muscle strength or changes in protein expression of factors involved in muscle protein turnover, in quadriceps fiber CSA, and in the ex vivo maximal strength. In view of these data, we

suggest that gut microbiota only slightly influences skeletal muscle mass in healthy conditions.

Gut Microbiota and Muscle Endurance

It has been recently proposed that gut microbiota could affect physical performance (15). For instance, the diversity of gut microorganisms is higher in professional athletes (16). In addition, endurance performance is more enhanced in conventionalized and specific pathogen-free (SPF) mice than in GF mice (34). Several skeletal muscle-independent factors can alter the endurance performance, including cardiovascular deficiency, insufficient muscle capillarity, central fatigue, or pain (27, 31, 50, 53). To determine the specific impact of gut microbiota modulation on skeletal muscle, we performed, in addition to in vivo running tests, ex vivo muscle contractility tests. We observed in both experimental conditions a negative effect of gut microbiota depletion on muscle endurance, fully reversed by natural reseeding. Altogether, the ex vivo results confirm that gut microbiota specifically and directly affect muscle endurance.

Skeletal muscle endurance can be affected by several muscle alterations, including changes in muscle contractile phenotype, mitochondrial biogenesis, and/or reduction in substrate availability (22). Interestingly, after transplantation of gut microbiota from obese or lean pigs to GF mice, these mice replicated the skeletal muscle fiber characteristics and lipid metabolic profiles of the donor (70). Here, the absence of significant modifications in the proportion of the different MHC isoforms in the ATB group excludes major effects of microbiota changes on the muscle contractile phenotype. Bäckhed et al. (3) observed that, in GF mice, AMPK activity is increased in liver and skeletal muscle and suggested that this adaptation is a key mechanism by which GF mice are better protected from obesity. In our study, however, we did not find any modification in skeletal muscles in the activity of AMPK, the expression of peroxisome proliferator-activated receptor coactivator-1α, and mitochondrial DNA content in skeletal muscle of ATB mice. This suggests that mitochondrial biogenesis remained unchanged in ATB mice and therefore that endurance alteration is probably not the result of reduction of the maximal muscle oxygen consumption capacity. Such muscle metabolic discrepancies between ATB mice and GF mice could be because of differences in the duration of skeletal muscle exposure to a systemic environment with depleted gut microbiota.

Gut Microbiota Modulation Targets Muscle Glycogen Availability

Muscle endurance also depends on metabolic parameters, including substrate availability in skeletal muscle, such as glycogen and triglycerides, two key energetic substrates that regulate muscle capacity during prolonged strenuous exercise (28, 32). Interestingly, GF mice exhibit higher gut Fiaf expression compared with conventionalized mice, leading among others to a reduction of triglyceride storage in peripheral tissues, including liver (2). Fiaf is a glycoprotein recognized to also promote fatty acid oxidation through AMPK activation in skeletal muscle and to attenuate muscle lipid uptake by inhibiting lipoprotein lipase activity (13, 57). Here, we confirmed the data of Bäckhed and colleagues by showing that gut Fiaf gene expression is modulated by the lack/presence of gut bacteria. However, these results were not associated in skeletal muscle with changes in *1*) free fatty acid transporter gene expression (*Cd36*, *Cpt1*), *2*) AMPK activation, and *3*) muscle triglyceride content. Altogether, these findings suggest that muscle lipid metabolism is unlikely to play a major role in alterations of muscle endurance observed after gut microbiota modulation.

Our data on glucose homeostasis both in ileum and skeletal muscle open some interesting hypotheses. Indeed, in ileum, *Gpr41* and *Sglt1* gene expression patterns followed the skeletal muscle endurance capacity (i.e., decrease in bacteria-depleted conditions reversible upon natural reseeding). Dependent to metabolites derived from gut bacteria, Gpr41 contributes to enteroendocrine cell activation and, by its action on glucagon-like peptide 1 release, regulates glucose-mediated insulin secretion (30, 68). In the same line, we observed the modulation of expression of *Sglt1* gene, encoding a sodium-glucose cotransporter located in enterocytes, which could reflect glucose homeostasis dysregulation in the intestinal tract. Overall, these results are in agreement with previous studies using antibiotic-induced microbiome depletion and showing a modulation of gene expression programs required for glucose homeostasis both in intestine and liver (18, 58, 72). Zarrinpar and colleagues also highlighted that antibiotics, by depleting gut bacteria in colon, reduce SCFA production and deprive colonocytes from butyrate, their main fuel source, and this results in lowering serum glucose and improving insulin sensitivity (72). This potential mechanism may contribute to the reduction of muscle glycogen store reported in the present study, since glycogen storage depends on both carbohydrate availability and uptake (39). Because reduction of glycogen content affects muscle fatigue in both in vivo and ex vivo conditions (51), the muscle glycogen depletion observed in ATB mice could be one of the key mechanisms to explain the muscle endurance reduction in these animals. Furthermore, the restoration of glycogen content to values close to CTL mice after natural reseeding reinforced this hypothesis. Interestingly, we demonstrated the same muscle glycogen level reduction in GF mice, another recognized model of gut microbiota depletion, compared with GF-reseeded mice (data not shown). All of these findings finally suggest that the reduction of energetic substrate availability, especially glucose, because of intestinal microbiota disruption could induce a reduction of muscle glycogen storage to maintain glucose homeostasis, translating in skeletal muscle endurance impairment.

To conclude, our results indicate for the first time that gut bacteria are critical for optimal muscle function in mice at least in part by altering glucose homeostasis regulation. How could we translate these finding in humans? The presence of a gut-muscle axis in the pathogenesis of age-related sarcopenia in humans has been proposed recently based on very promising results (67). The interplay between microbiome and skeletal muscle has been highlighted by Siddhart and colleagues (64) who demonstrated that age-related changes of gut microbiome are associated with the physiological decline of musculoskeletal function. Future studies will be needed to identify the bacterial species and/or the underlying mechanisms and the putative metabolites that contribute to the functional link between gut microbiota and skeletal muscle. Our work opens promising perspectives to develop new therapeutic strategies

based on gut microbiota modulation for muscle-related diseases, muscle disuse, and sport training.

ACKNOWLEDGMENTS

We are grateful to the Genotoul Bioinformatics Facility, Toulouse Midi-Pyrenees (BioinfoGenotoul), for providing help, computing, and storage resources. We thank the animal staff from the METAMUS DMEM platform facility, which belongs to the "Montpellier Animal Facilities Network." We also acknowledge the MRI imaging facility, which is a part of the national bioimaging infrastructure supported by the French National Research Agency (ANR-10-INBS-04, Investments for the future).

GRANTS

The work was supported by INRA and Brittany Council and partially supported by an AlimH department grant. This work was also supported by the Centre National d'Etudes Spatiales.

DISCLOSURES

No conflicts of interest, financial or otherwise, are declared by the authors.

AUTHOR CONTRIBUTIONS

C.K.-R. conceived and designed research; K.N., M.J., B.G., N.B., B.V., M.P., L.L.-O., C.B., P.L., and C.K.-R. performed experiments; K.N., M.J., B.G., B.V., L.L.-O., O.R., M.M., V.O., P.L., F.D., and C.K.-R. analyzed data; K.N., M.J., B.G., O.R., M.M., A.B., V.O., P.L., F.D., and C.K.-R. interpreted results of experiments; K.N., M.J., P.L., and C.K.-R. prepared figures; K.N., A.B., V.O., F.D., and C.K.-R. drafted manuscript; K.N., B.G., A.B., V.O., F.D., and C.K.-R. edited and revised manuscript; K.N., M.J., B.G., M.P., L.L.-O., C.B., O.R., M.M., A.B., V.O., P.L., F.D., and C.K.-R. approved final version of manuscript.

REFERENCES

1. **Adamo KB, Graham TE.** Comparison of traditional measurements with macroglycogen and proglycogen analysis of muscle glycogen. *J Appl Physiol (1985)* 84: 908–913, 1998. doi:10.1152/jappl.1998.84.3.908.
2. **Bäckhed F, Ding H, Wang T, Hooper LV, Koh GY, Nagy A, Semenkovich CF, Gordon JI.** The gut microbiota as an environmental factor that regulates fat storage. *Proc Natl Acad Sci USA* 101: 15718–15723, 2004. doi:10.1073/pnas.0407076101.
3. **Bäckhed F, Manchester JK, Semenkovich CF, Gordon JI.** Mechanisms underlying the resistance to diet-induced obesity in germ-free mice. *Proc Natl Acad Sci USA* 104: 979–984, 2007. doi:10.1073/pnas.0605374104.
4. **Bindels LB, Beck R, Schakman O, Martin JC, De Backer F, Sohet FM, Dewulf EM, Pachikian BD, Neyrinck AM, Thissen J-P, Verrax J, Calderon PB, Pot B, Grangette C, Cani PD, Scott KP, Delzenne NM.** Restoring specific lactobacilli levels decreases inflammation and muscle atrophy markers in an acute leukemia mouse model. *PLoS One* 7: e37971, 2012. doi:10.1371/journal.pone.0037971.
5. **Bindels LB, Delzenne NM.** Muscle wasting: the gut microbiota as a new therapeutic target? *Int J Biochem Cell Biol* 45: 2186–2190, 2013. doi:10.1016/j.biocel.2013.06.021.
6. **Bindels LB, Neyrinck AM, Salazar N, Taminiau B, Druart C, Muccioli GG, François E, Blecker C, Richel A, Daube G, Mahillon J, de los Reyes-Gavilán CG, Cani PD, Delzenne NM.** Non digestible oligosaccharides modulate the gut microbiota to control the development of leukemia and associated cachexia in mice. *PLoS One* 10: e0131009, 2015. doi:10.1371/journal.pone.0131009.
7. **Bligh EG, Dyer WJ.** A rapid method of total lipid extraction and purification. *Can J Biochem Physiol* 37: 911–917, 1959. doi:10.1139/y59-099.
8. **Bokulich NA, Subramanian S, Faith JJ, Gevers D, Gordon JI, Knight R, Mills DA, Caporaso JG.** Quality-filtering vastly improves diversity estimates from Illumina amplicon sequencing. *Nat Methods* 10: 57–59, 2013. doi:10.1038/nmeth.2276.
9. **Boursier J, Mueller O, Barret M, Machado M, Fizanne L, Araujo-Perez F, Guy CD, Seed PC, Rawls JF, David LA, Hunault G, Oberti F, Calès P, Diehl AM.** The severity of nonalcoholic fatty liver disease is associated with gut dysbiosis and shift in the metabolic function of the gut microbiota. *Hepatology* 63: 764–775, 2016. doi:10.1002/hep.28356.
10. **Britto FA, Cortade F, Belloum Y, Blaquière M, Gallot YS, Docquier A, Pagano AF, Jublanc E, Bendridi N, Koechlin-Ramonatxo C, Chabi B, Francaux M, Casas F, Freyssenet D, Rieusset J, Giorgetti-Peraldi S, Carnac G, Ollendorff V, Favier FB.** Glucocorticoid-dependent REDD1 expression reduces muscle metabolism to enable adaptation under energetic stress. *BMC Biol* 16: 65, 2018. doi:10.1186/s12915-018-0525-4.
11. **Bustin SA, Benes V, Garson JA, Hellemans J, Huggett J, Kubista M, Mueller R, Nolan T, Pfaffl MW, Shipley GL, Vandesompele J, Wittwer CT.** The MIQE guidelines: minimum information for publication of quantitative real-time PCR experiments. *Clin Chem* 55: 611–622, 2009. doi:10.1373/clinchem.2008.112797.
12. **Catoire M, Alex S, Paraskevopulos N, Mattijssen F, Evers-van Gogh I, Schaart G, Jeppesen J, Kneppers A, Mensink M, Voshol PJ, Olivecrona G, Tan NS, Hesselink MKC, Berbée JF, Rensen PCN, Kalkhoven E, Schrauwen P, Kersten S.** Fatty acid-inducible ANGPTL4 governs lipid metabolic response to exercise. *Proc Natl Acad Sci USA* 111: E1043–E1052, 2014. doi:10.1073/pnas.1400889111.
13. **Chang H, Kwon O, Shin M-S, Kang GM, Leem YH, Lee CH, Kim SJ, Roh E, Kim H-K, Youn B-S, Kim M-S.** Role of Angptl4/Fiaf in exercise-induced skeletal muscle AMPK activation. *J Appl Physiol (1985)* 125: 715–722, 2018. doi:10.1152/japplphysiol.00984.2016.
14. **Chen Y-M, Wei L, Chiu Y-S, Hsu Y-J, Tsai T-Y, Wang M-F, Huang C-C.** Lactobacillus plantarum TWK10 supplementation improves exercise performance and increases muscle mass in mice. *Nutrients* 8: 205, 2016. doi:10.3390/nu8040205.
15. **Clark A, Mach N.** The crosstalk between the gut microbiota and mitochondria during exercise. *Front Physiol* 8: 319, 2017. doi:10.3389/fphys.2017.00319.
16. **Clarke SF, Murphy EF, O'Sullivan O, Lucey AJ, Humphreys M, Hogan A, Hayes P, O'Reilly M, Jeffery IB, Wood-Martin R, Kerins DM, Quigley E, Ross RP, O'Toole PW, Molloy MG, Falvey E, Shanahan F, Cotter PD.** Exercise and associated dietary extremes impact on gut microbial diversity. *Gut* 63: 1913–1920, 2014. doi:10.1136/gutjnl-2013-306541.
17. **Clemente JC, Ursell LK, Parfrey LW, Knight R.** The impact of the gut microbiota on human health: an integrative view. *Cell* 148: 1258–1270, 2012. doi:10.1016/j.cell.2012.01.035.
18. **Cresci GA, Thangaraju M, Mellinger JD, Liu K, Ganapathy V.** Colonic gene expression in conventional and germ-free mice with a focus on the butyrate receptor GPR109A and the butyrate transporter SLC5A8. *J Gastrointest Surg* 14: 449–461, 2010. doi:10.1007/s11605-009-1045-x.
19. **Demangel R, Treffel L, Py G, Brioche T, Pagano AF, Bareille MP, Beck A, Pessemesse L, Candau R, Gharib C, Chopard A, Millet C.** Early structural and functional signature of 3-day human skeletal muscle disuse using the dry immersion model. *J Physiol* 595: 4301–4315, 2017. doi:10.1113/JP273895.
20. **Derbré F, Droguet M, Léon K, Troadec S, Pennec J-P, Giroux-Metges M-A, Rannou F.** Single muscle immobilization decreases single-fibre myosin heavy chain polymorphism: possible involvement of p38 and JNK MAP kinases. *PLoS One* 11: e0158630, 2016. doi:10.1371/journal.pone.0158630.
21. **Dinan TG, Cryan JF.** Gut instincts: microbiota as a key regulator of brain development, ageing and neurodegeneration. *J Physiol* 595: 489–503, 2017. doi:10.1113/JP273106.
22. **Egan B, Zierath JR.** Exercise metabolism and the molecular regulation of skeletal muscle adaptation. *Cell Metab* 17: 162–184, 2013. doi:10.1016/j.cmet.2012.12.012.
23. **Escudié F, Auer L, Bernard M, Mariadassou M, Cauquil L, Vidal K, Maman S, Hernandez-Raquet G, Combes S, Pascal G.** FROGS: find, rapidly, OTUs with Galaxy solution. *Bioinformatics* 34: 1287–1294, 2018. doi:10.1093/bioinformatics/btx791.
24. **Evans WJ.** Skeletal muscle loss: cachexia, sarcopenia, and inactivity. *Am J Clin Nutr* 91: 1123S–1127S, 2010. doi:10.3945/ajcn.2010.28608A.
25. **Fröhlich EE, Farzi A, Mayerhofer R, Reichmann F, Jačan A, Wagner B, Zinser E, Bordag N, Magnes C, Fröhlich E, Kashofer K, Gorkiewicz G, Holzer P.** Cognitive impairment by antibiotic-induced gut dysbiosis: Analysis of gut microbiota-brain communication. *Brain Behav Immun* 56: 140–155, 2016. doi:10.1016/j.bbi.2016.02.020.
26. **Furet J-P, Firmesse O, Gourmelon M, Bridonneau C, Tap J, Mondot S, Doré J, Corthier G.** Comparative assessment of human and farm animal faecal microbiota using real-time quantitative PCR. *FEMS Microbiol Ecol* 68: 351–362, 2009. doi:10.1111/j.1574-6941.2009.00671.x.
27. **Gonglach AR, Ade CJ, Bemben MG, Larson RD, Black CD.** Muscle pain as a regulator of cycling intensity: effect of caffeine ingestion. *Med Sci Sports Exerc* 48: 287–296, 2016. doi:10.1249/MSS.0000000000000767.

28. **Goodpaster BH, He J, Watkins S, Kelley DE.** Skeletal muscle lipid content and insulin resistance: evidence for a paradox in endurance-trained athletes. *J Clin Endocrinol Metab* 86: 5755–5761, 2001. doi:10.1210/jcem.86.12.8075.
29. **Guo X, Xia X, Tang R, Zhou J, Zhao H, Wang K.** Development of a real-time PCR method for Firmicutes and Bacteroidetes in faeces and its application to quantify intestinal population of obese and lean pigs. *Lett Appl Microbiol* 47: 367–373, 2008. doi:10.1111/j.1472-765X.2008.02408.x.
30. **Hansen TH, Gøbel RJ, Hansen T, Pedersen O.** The gut microbiome in cardio-metabolic health. *Genome Med* 7: 33, 2015. doi:10.1186/s13073-015-0157-z.
31. **Hermansen L, Ekblom B, Saltin B.** Cardiac output during submaximal and maximal treadmill and bicycle exercise. *J Appl Physiol* 29: 82–86, 1970. doi:10.1152/jappl.1970.29.1.82.
32. **Hermansen L, Hultman E, Saltin B.** Muscle glycogen during prolonged severe exercise. *Acta Physiol Scand* 71: 129–139, 1967. doi:10.1111/j.1748-1716.1967.tb03719.x.
33. **Houghton MJ, Kerimi A, Mouly V, Tumova S, Williamson G.** Gut microbiome catabolites as novel modulators of muscle cell glucose metabolism. *FASEB J* 33: 1887–1898, 2018. doi:10.1096/fj.201801209R.
34. **Hsu YJ, Chiu CC, Li YP, Huang WC, Huang YT, Huang CC, Chuang HL.** Effect of intestinal microbiota on exercise performance in mice. *J Strength Cond Res* 29: 552–558, 2015. doi:10.1519/JSC.0000000000000644.
35. **Jäger R, Shields KA, Lowery RP, De Souza EO, Partl JM, Hollmer C, Purpura M, Wilson JM.** Probiotic Bacillus coagulans GBI-30, 6086 reduces exercise-induced muscle damage and increases recovery. *PeerJ* 4: e2276, 2016. doi:10.7717/peerj.2276.
36. **Jäger S, Handschin C, St-Pierre J, Spiegelman BM.** AMP-activated protein kinase (AMPK) action in skeletal muscle via direct phosphorylation of PGC-1alpha. *Proc Natl Acad Sci USA* 104: 12017–12022, 2007. doi:10.1073/pnas.0705070104.
37. **Janssen AWF, Kersten S.** Potential mediators linking gut bacteria to metabolic health: a critical view. *J Physiol* 595: 477–487, 2017. doi:10.1113/JP272476.
38. **Jansson E.** Acid soluble and insoluble glycogen in human skeletal muscle. *Acta Physiol Scand* 113: 337–340, 1981. doi:10.1111/j.1748-1716.1981.tb06904.x.
39. **Jensen TE, Richter EA.** Regulation of glucose and glycogen metabolism during and after exercise. *J Physiol* 590: 1069–1076, 2012. doi:10.1113/jphysiol.2011.224972.
40. **Levy LB, Welch AA.** Implications of skeletal muscle loss for public health nutrition messages: a brief report. *Proc Nutr Soc* 74: 426–429, 2015. doi:10.1017/S0029665115002116.
41. **Linninge C, Ahrné S, Molin G.** Pre-treatment with antibiotics and Escherichia coli to equalize the gut microbiota in conventional mice. *Antonie van Leeuwenhoek* 107: 149–156, 2015. doi:10.1007/s10482-014-0312-3.
42. **Lundberg R, Toft MF, August B, Hansen AK, Hansen CHF.** Antibiotic-treated versus germ-free rodents for microbiota transplantation studies. *Gut Microbes* 7: 68–74, 2016. doi:10.1080/19490976.2015.1127463.
43. **Lunde PK, Dahlstedt AJ, Bruton JD, Lännergren J, Thorén P, Sejersted OM, Westerblad H.** Contraction and intracellular Ca(2+) handling in isolated skeletal muscle of rats with congestive heart failure. *Circ Res* 88: 1299–1305, 2001. doi:10.1161/hh1201.092041.
44. **MacDonald PE, El-Kholy W, Riedel MJ, Salapatek AMF, Light PE, Wheeler MB.** The multiple actions of GLP-1 on the process of glucose-stimulated insulin secretion. *Diabetes* 51, *Suppl* 3: S434–S442, 2002. doi:10.2337/diabetes.51.2007.S434.
45. **Magoč T, Salzberg SL.** FLASH: fast length adjustment of short reads to improve genome assemblies. *Bioinformatics* 27: 2957–2963, 2011. doi:10.1093/bioinformatics/btr507.
46. **Mahé F, Rognes T, Quince C, de Vargas C, Dunthorn M.** Swarm v2: highly-scalable and high-resolution amplicon clustering. *PeerJ* 3: e1420, 2015. doi:10.7717/peerj.1420.
47. **Martin M.** Cutadapt removes adapter sequences from high-throughput sequencing reads. *EMBnet.journal* 17: 10–12, 2011. doi:10.14806/ej.17.1.200.
48. **McMurdie PJ, Holmes S.** phyloseq: an R package for reproducible interactive analysis and graphics of microbiome census data. *PLoS One* 8: e61217, 2013. doi:10.1371/journal.pone.0061217.
49. **Nakanishi Y, Murashima K, Ohara H, Suzuki T, Hayashi H, Sakamoto M, Fukasawa T, Kubota H, Hosono A, Kono T, Kaminogawa S, Benno Y.** Increase in terminal restriction fragments of Bacteroidetes-derived 16S rRNA genes after administration of short-chain fructooligosaccharides. *Appl Environ Microbiol* 72: 6271–6276, 2006. doi:10.1128/AEM.00477-06.
50. **Olfert IM, Howlett RA, Tang K, Dalton ND, Gu Y, Peterson KL, Wagner PD, Breen EC.** Muscle-specific VEGF deficiency greatly reduces exercise endurance in mice. *J Physiol* 587: 1755–1767, 2009. doi:10.1113/jphysiol.2008.164384.
51. **Ørtenblad N, Westerblad H, Nielsen J.** Muscle glycogen stores and fatigue. *J Physiol* 591: 4405–4413, 2013. doi:10.1113/jphysiol.2013.251629.
52. **Palaferri Schieber AM, Lee YM, Chang MW, Leblanc M, Collins B, Downes M, Evans RM, Ayres JS.** Disease tolerance mediated by commensal E. coli via inflammasome and IGF-1 signaling. *Science* 350: 558–563, 2015. doi:10.1126/science.aac6468.
53. **Piedimonte A, Benedetti F, Carlino E.** Placebo-induced decrease in fatigue: evidence for a central action on the preparatory phase of movement. *Eur J Neurosci* 41: 492–497, 2015. doi:10.1111/ejn.12806.
54. **Ploquin C, Chabi B, Fouret G, Vernus B, Feillet-Coudray C, Coudray C, Bonnieu A, Ramonatxo C.** Lack of myostatin alters intermyofibrillar mitochondria activity, unbalances redox status, and impairs tolerance to chronic repetitive contractions in muscle. *Am J Physiol Endocrinol Metab* 302: E1000–E1008, 2012. doi:10.1152/ajpendo.00652.2011.
55. **Quast C, Pruesse E, Yilmaz P, Gerken J, Schweer T, Yarza P, Peplies J, Glöckner FO.** The SILVA ribosomal RNA gene database project: improved data processing and web-based tools. *Nucleic Acids Res* 41: D590–D596, 2013. doi:10.1093/nar/gks1219.
56. **Reikvam DH, Erofeev A, Sandvik A, Grcic V, Jahnsen FL, Gaustad P, McCoy KD, Macpherson AJ, Meza-Zepeda LA, Johansen F-E.** Depletion of murine intestinal microbiota: effects on gut mucosa and epithelial gene expression. *PLoS One* 6: e17996, 2011. doi:10.1371/journal.pone.0017996.
57. **Robciuc MR, Skrobuk P, Anisimov A, Olkkonen VM, Alitalo K, Eckel RH, Koistinen HA, Jauhiainen M, Ehnholm C.** Angiopoietin-like 4 mediates PPAR delta effect on lipoprotein lipase-dependent fatty acid uptake but not on beta-oxidation in myotubes. *PLoS One* 7: e46212, 2012. doi:10.1371/journal.pone.0046212.
58. **Rodrigues RR, Greer RL, Dong X, DSouza KN, Gurung M, Wu JY, Morgun A, Shulzhenko N.** Antibiotic-induced alterations in gut microbiota are associated with changes in glucose metabolism in healthy mice. *Front Microbiol* 8: 2306, 2017. doi:10.3389/fmicb.2017.02306.
59. **Rognes T, Flouri T, Nichols B, Quince C, Mahé F.** VSEARCH: a versatile open source tool for metagenomics. *PeerJ* 4: e2584, 2016. doi:10.7717/peerj.2584.
60. **Ryall JG, Gregorevic P, Plant DR, Sillence MN, Lynch GS.** Beta 2-agonist fenoterol has greater effects on contractile function of rat skeletal muscles than clenbuterol. *Am J Physiol Regul Integr Comp Physiol* 283: R1386–R1394, 2002. doi:10.1152/ajpregu.00324.2002.
61. **Schmittgen TD, Livak KJ.** Analyzing real-time PCR data by the comparative C(T) method. *Nat Protoc* 3: 1101–1108, 2008. doi:10.1038/nprot.2008.73.
62. **Schuijt TJ, Lankelma JM, Scicluna BP, de Sousa e Melo F, Roelofs JJ, de Boer JD, Hoogendijk AJ, de Beer R, de Vos A, Belzer C, de Vos WM, van der Poll T, Wiersinga WJ.** The gut microbiota plays a protective role in the host defence against pneumococcal pneumonia. *Gut* 65: 575–583, 2016. doi:10.1136/gutjnl-2015-309728.
63. **Sekirov I, Russell SL, Antunes LCM, Finlay BB.** Gut microbiota in health and disease. *Physiol Rev* 90: 859–904, 2010. doi:10.1152/physrev.00045.2009.
64. **Siddharth J, Chakrabarti A, Pannérec A, Karaz S, Morin-Rivron D, Masoodi M, Feige JN, Parkinson SJ.** Aging and sarcopenia associate with specific interactions between gut microbes, serum biomarkers and host physiology in rats. *Aging (Albany NY)* 9: 1698–1720, 2017. doi:10.18632/aging.101262.
65. **Steves CJ, Bird S, Williams FM, Spector TD.** The microbiome and musculoskeletal conditions of aging: a review of evidence for impact and potential therapeutics. *J Bone Miner Res* 31: 261–269, 2016. doi:10.1002/jbmr.2765.
66. **Talmadge RJ, Roy RR.** Electrophoretic separation of rat skeletal muscle myosin heavy-chain isoforms. *J Appl Physiol (1985)* 75: 2337–2340, 1993. doi:10.1152/jappl.1993.75.5.2337.
67. **Ticinesi A, Lauretani F, Milani C, Nouvenne A, Tana C, Del Rio D, Maggio M, Ventura M, Meschi T.** Aging gut microbiota at the cross-road between nutrition, physical frailty, and sarcopenia: is there a gut-muscle axis? *Nutrients* 9: E1303, 2017. doi:10.3390/nu9121303.

68. **Tolhurst G, Heffron H, Lam YS, Parker HE, Habib AM, Diakogiannaki E, Cameron J, Grosse J, Reimann F, Gribble FM.** Short-chain fatty acids stimulate glucagon-like peptide-1 secretion via the G-protein-coupled receptor FFAR2. *Diabetes* 61: 364–371, 2012. doi:10.2337/db11-1019.
69. **Varian BJ, Goureshetti S, Poutahidis T, Lakritz JR, Levkovich T, Kwok C, Teliousis K, Ibrahim YM, Mirabal S, Erdman SE.** Beneficial bacteria inhibit cachexia. *Oncotarget* 7: 11803–11816, 2016. doi:10.18632/oncotarget.7730.
70. **Yan H, Diao H, Xiao Y, Li W, Yu B, He J, Yu J, Zheng P, Mao X, Luo Y, Zeng B, Wei H, Chen D.** Gut microbiota can transfer fiber characteristics and lipid metabolic profiles of skeletal muscle from pigs to germ-free mice. *Sci Rep* 6: 31786, 2016. doi:10.1038/srep31786.
71. **Yu LC-H, Wang J-T, Wei S-C, Ni Y-H.** Host-microbial interactions and regulation of intestinal epithelial barrier function: from physiology to pathology. *World J Gastrointest Pathophysiol* 3: 27–43, 2012. doi:10.4291/wjgp.v3.i1.27.
72. **Zarrinpar A, Chaix A, Xu ZZ, Chang MW, Marotz CA, Saghatelian A, Knight R, Panda S.** Antibiotic-induced microbiome depletion alters metabolic homeostasis by affecting gut signaling and colonic metabolism. *Nat Commun* 9: 2872, 2018. doi:10.1038/s41467-018-05336-9.